Progress report on the optical system for closed-loop testing of the multiple mirror telescope adaptive secondary mirror

Roland J. Sarlot, Cynthia J. Bresloff, James H. Burge, Bruce C. Fitz-Patrick, Patrick C. McGuire, Brian L. Stamper, Chun Yu Zhao

Steward Observatory, University of Arizona, Tucson, AZ, 85721, USA

ABSTRACT

Steward Observatory is completing the manufacture of a deformable f/15 secondary mirror for the 6.5m Multiple Mirror Telescope conversion that will, along with the wavefront sensing system, compensate for atmospheric turbulence. A potential difficulty of an adaptive secondary mirror is the ability to verify the commanded mirror shapes of a large convex deformable surface. An optical design is presently being implemented to test the deformable mirror's closed loop control system by optically projecting an artificial star to simulate starlight in the actual telescope. The test system has been designed to verify the control system by fitting into both a laboratory test structure as well as the telescope support structure itself. The optical design relies on two wavelength computer generated holograms used to remove spherical aberration as well as aid in the alignment of the test system optics by projecting alignment patterns.

Keywords: adaptive secondary, aspheric testing, Multiple Mirror Telescope, Shimmulator

1. INTRODUCTION

The University of Arizona's 6.5m Multiple Mirror Telescope (MMT) conversion will include an adaptive optic system designed to correct atmospheric turbulence. The compensation is accomplished with a 640mm diameter by 1.6mm thick convex hyperboloidal f/15 secondary with 336 voice coil electromagnetic actuators directly mounted to the back of the mirror. These actuators will deform the mirror based on inputs from the guide star/wavefront sensing system and reconstruction software.[1]

An optical design was proposed to test the adaptive optic system in closed-loop and to verify the systems ability for wavefront compensation.[2] The design required a solution to provide dual wavelength simulation of starlight reflecting off the secondary mirror analogous to the reflection in the telescope. This test setup implemented a method to induce atmospheric turbulence as well as measure the system's ability to adapt by way of a fiber fed interferometer. In this manner, the wavefront sensor, computers and reconstructing software can be tested and calibrated off telescope and not waste valuable telescope time for instrument debugging.

The closed-loop optical design was guided under multiple constraints. In particular, chromatic light from the secondary mirror was required to focus at the Cassegrain focal plane in the same focal ratio with pupil mapping limited to less than 2mm at the secondary for proper actuator influence. The system must perform equally with a preliminary spherical test as well as the aspherical mirror and operate in the laboratory as well as in-situ. Additionally, the system includes two counter rotating plates simulating Kolmogorov turbulence. By changing the plates' distances from the source, the magnitude and effective spatial resolution can be adjusted and simulated.[3]

2. OPTICAL DESIGN-BACKGROUND

Since the optical design is a starlight and atmospheric turbulence simulator, it is colloquially termed the Shimmulator, and its raytrace is outlined in Figure 1. The same test setup is required to test three mirrors- a rigid spherical body, a thin shell spherical prototype and the thin shell aspherical secondary telescope mirror. For all tests, a fiber fed 594nm and 1.5μm point source is projected through the spinning atmospheric turbulence generator plates and passes through a fused silica substrate with a computer generated hologram written on the back surface before reflecting off the beam splitter and passing through the 170mm diameter doublet. Nearly 8m away, before the light reflects off the secondary, there are two 700 mm diameter BK7 lenses. These lenses essentially neutralize the convexity of the secondary and guide the light back towards the image plane. The doublet acts as a pupil mapping compensator for both wavelengths. Detail of the large lenses and optical components near the source end is shown in Figure 2.

Part of the SPIE Conference on Current Developments in Optical Design and Optical Engineering VIII • Denver, Colorado • July 1999
SPIE Vol. 3779 • 0277-786X/99/$10.00

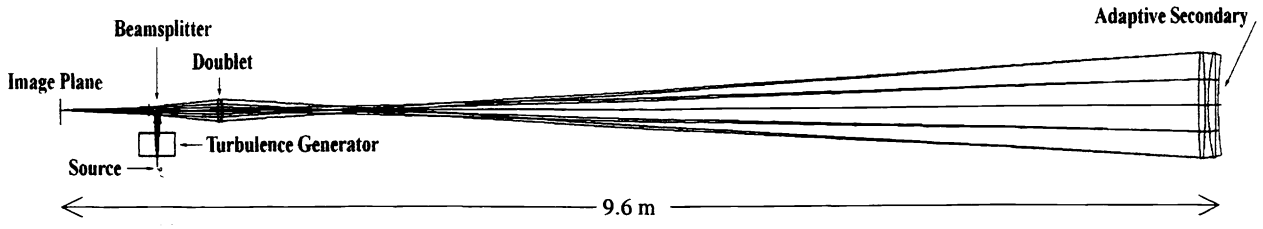

Figure 1. Full Shimmulator test setup. Rays emerge from the fiber optic point source through the turbulence generator, computer generated hologram and reflected off of the adaptive secondary back through the doublet towards the image plane.

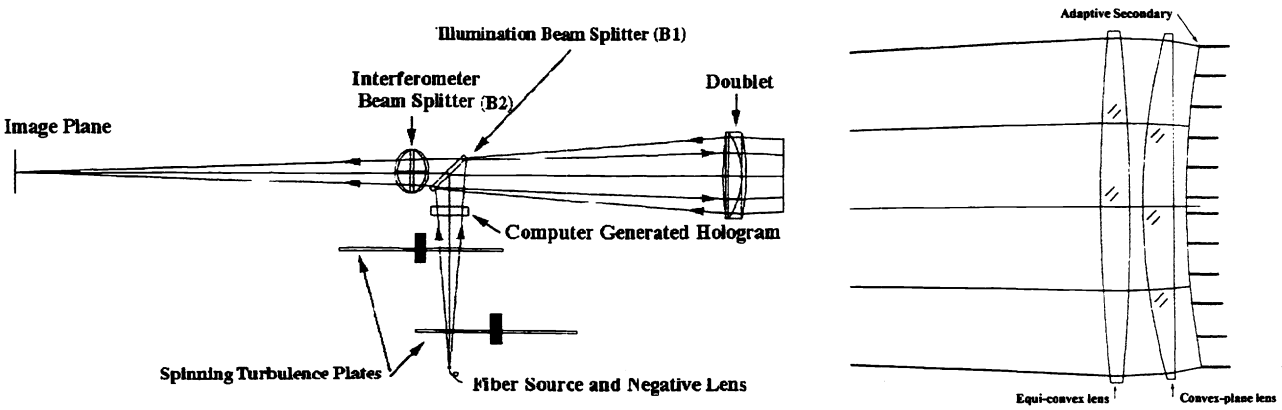

Figure 2. Optical element detail. Specifics of the source optics on the left are shown, with the 700mm lenses and adaptive secondary drawn to scale on the right.

Although there is a 24mm difference in the back focal distance, the optical paths for both wavelengths are completely different. Figure 3 illustrates the beam paths for both wavelengths. Testing either the aspherical or the spherical secondary mirror does not require any changes in the optical setup other than a single change of holograms.

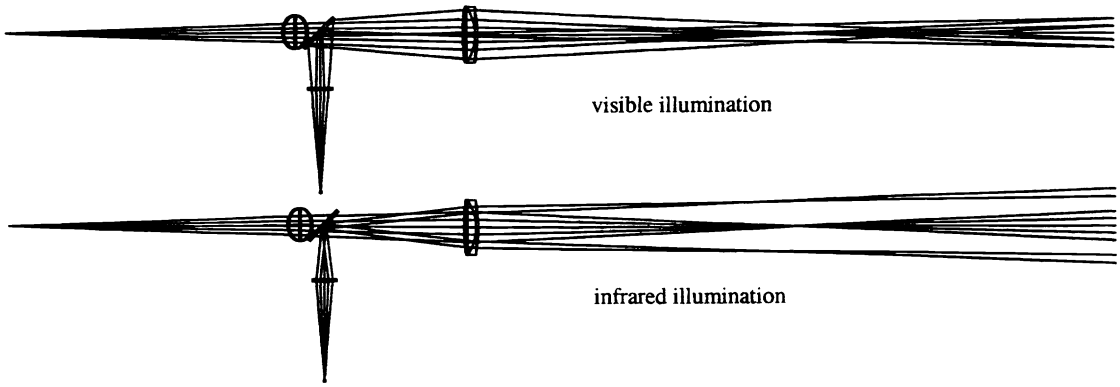

Figure 3. Spectral ray paths. The above two illustrations trace the ray paths for each illumination wavelength through the Shimmulator optical test. The ray paths through the configurations are significantly different yet the rays converge with equivalent focal ratio, mapping and location as the MMT Cassegrain f/15 focus.

Early on in the design phase, we realized that computer generated holograms (CGH) would effectively remove the large amounts of spherical aberration caused by the lenses and the secondary mirror. For the aspheric test system, approximately 4000 waves peak-to-valley of spherical aberration at 594 nm were present before the hologram was installed. With the hologram, less than 1/5 of a wave of coma remained with no residual spherical aberration. Three holograms were designed for

the Shimmulator: one for the adaptive spherical mirror, one for the adaptive aspherical secondary and one for verification purposes.

Another interesting feature designed into the computer generated holograms is multiplexing. Since the system is required to have dual wavelength operation and no element can be changed during testing, the holograms were designed for simultaneous two wavelength diffraction. To accomplish this task, two hologram prescriptions were written over the same central spherical-aberration-removing core and arranged such that each single wavelength hologram pattern alternates with the other pattern. This multiplexing of the two holograms was designed with a constant spacing between the alternating hologram prescriptions. The system imaging requirements demanded a 5.6 arcsecond field referenced back to the sky. Therefore, the hologram spacing for each wavelength was calculated such that the effects of multiplexing would lie outside the 5.6 arcsecond field stop. A 160μm spacing of the CGH patterns corresponds to a 5.6 arcsecond field at the image plane, therefore, all refracting non-first orders will not pass within this physical aperture. Figure 4 illustrates the alternating hologram patterns that incorporate multiplexing by emphasizing the 160 μm spacing between the two holograms in the central core and Figure 5 emphasizes the various diffracting order diameters as compared to the aperture.

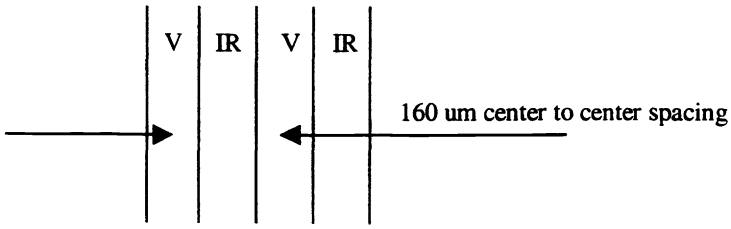

Figure 4. Hologram multiplexing. The ability to multiplex two holograms was incorporated by alternating the visible and infrared hologram patterns with a 160μm spacing between them. This spacing was determined so that stray orders would be outside the desired field.

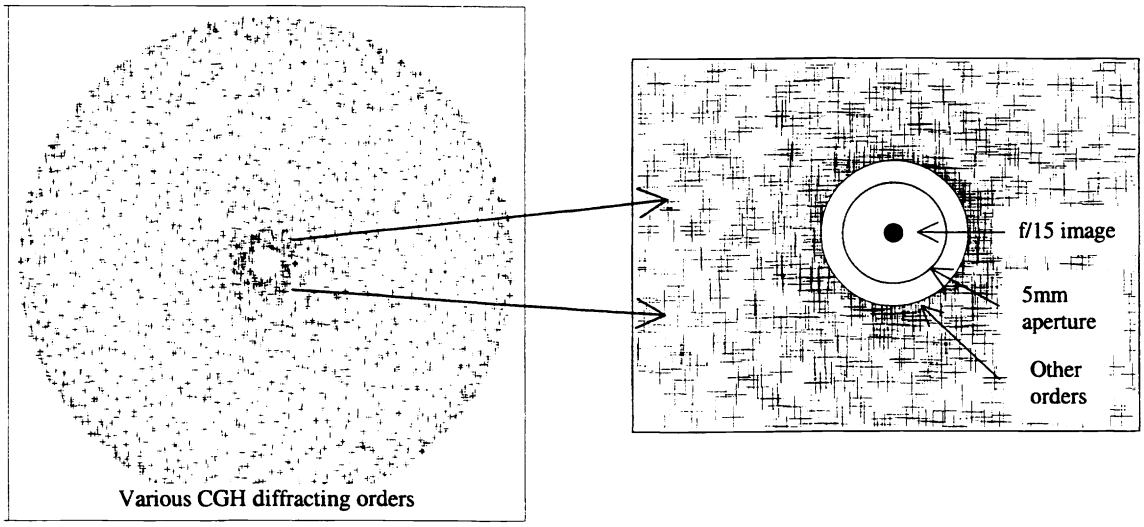

Figure 5. Stray diffracted orders. The illustration on the left is a spot diagram of multiple CGH orders at the nominal image plane. The magnified illustration on the right represents the various diameters of the diffracted holographic orders including the 5.6 arcsecond aperture and the principal diffracted order with excellent spherical aberration correction.

The multiplexing of the two holograms presented some difficulties such as crosstalk, a situation that causes stray orders of visible light to refract from the infrared CGH pattern and come to focus within the 5 mm diameter field stop positioned at the MMT f/15 focus. To eliminate this problem, the infrared CGH was left unwritten precisely over this region of overlap over the full inner radius of the main SA correcting section. Figure 6 shows the region where the infrared CGH pattern is left unwritten.

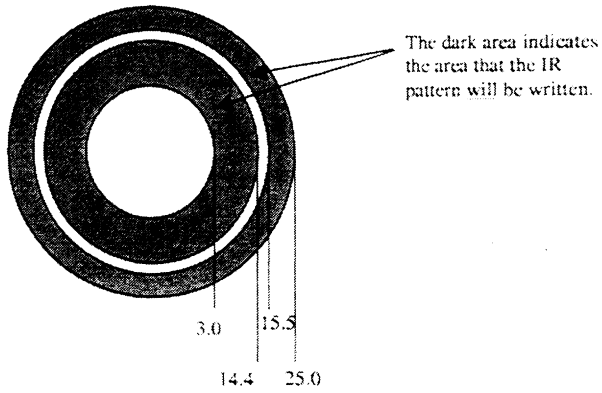

Figure 6. Eliminating crosstalk. The figure depicts the central spherical aberration hologram for the aspherical test. To avoid the problem of stray visible orders refracting through the infrared pattern, the infrared pattern is not written over the full pupil. The visible pattern is written over the full region from 3.0 mm to 25.0 mm where the infrared pattern is written over two separate regions leaving a void area, precisely vacating the area of crosstalk.

Another advantage employed by the computer generated holograms was the use of alignment patterns. These patterns project a crosshair of diffraction "dots" at precise locations perpendicular to the optical axis to aid in alignment of the most difficult component tolerances. In particular, they will be used for aiding decentration and spacing alignment where physical constraints hinder an inside micrometer. Five alignment patterns will be projected by the outside ring of alternating hologram prescriptions that surround the central 50 mm spherical aberration corrector. Figure 7 is the fundamental layout of the Shimmulator holograms.

To test the actuator control system, a 594nm phase shifting interferometer has been incorporated into the Shimmulator. The interferometer will be able to measure the adaptive secondary surface shapes as commanded by the software and quantify the mapping optics of the Shimmulator. Since the source for the Shimmulator for both wavelengths will be fiber-fed, the reference path of the interferometer will be coupled to the visible fiber source[4]. One fiber will feed the Shimmulator test system through the upper beamsplitter and represents the interferometer test path. The second phase-synced fiber will behave as the reference path and interfered with light passing through the upper beamsplitter and reflecting off of the lower beamsplitter for the test path. The interferometer will utilize an piezoelectric modulator for phase shifting and Durango phase shifting software with a Pulnix camera for image acquisition and phase measurement[5].

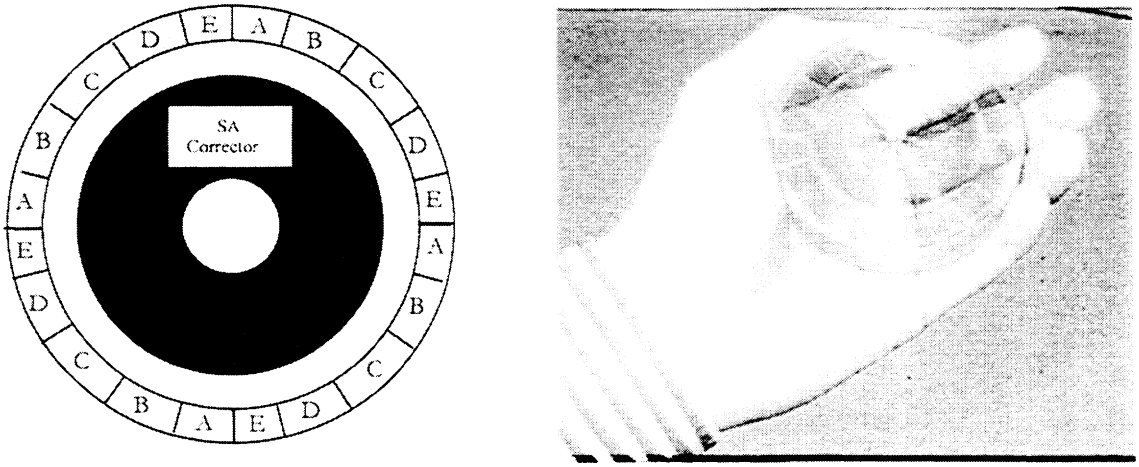

Figure 7. CGH patterns. The drawing illustrates the basic hologram layout with the five alignment patterns

(named with letters) rotating around the main spherical aberration correcting prescription. Each of the five alignment patterns is written onto the CGH substrate four times with the same pattern alternating a factor of 90 degrees from its "partners". On the right is a photo of the actual CGH for the aspheric secondary test.

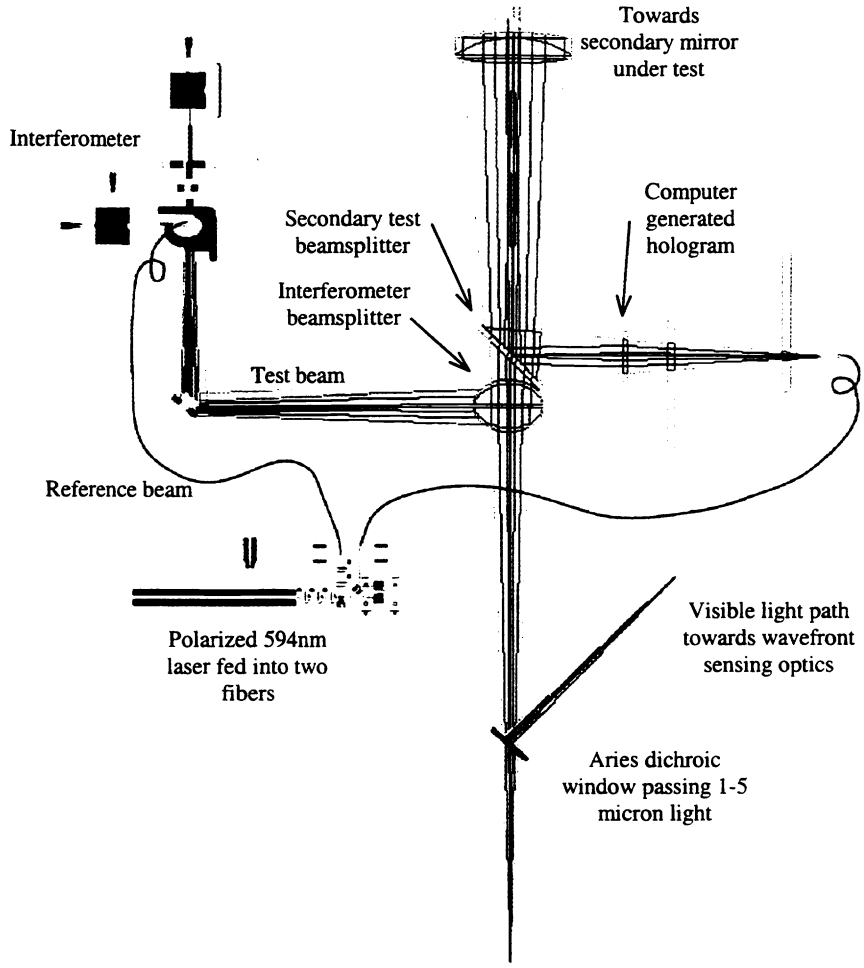

Figure 8. Schematic of the interferometer coupled within the optical test. The arrangement highlights the integration of the interferometer within the Shimmulator test setup. The laser source is split into two single mode optical fibers, one feeds the interferometer reference path and the other feeds the illumination test path. The wavefront sensing optics are not shown in the figure.

3. INSTALLATION

Currently the Shimmulator is in the first testing locale, the Steward Observatory Mirror Lab, imaging a solid body spherical test mirror. The goal of the first test is to align the test elements, integrate the wavefront sensor and measure the residual wavefront and distortion of the test system with the interferometer. Because of the long path length, two fold flats have been inserted within the beam to shorten the physical dimension. The test tower (see Figure 9) provides a support for the Shimmulator optics and integrates the wavefront sensing Top Box optics as well as providing a mounting flange for the main diffraction limited near infrared science instrument, ARIES[6,7].

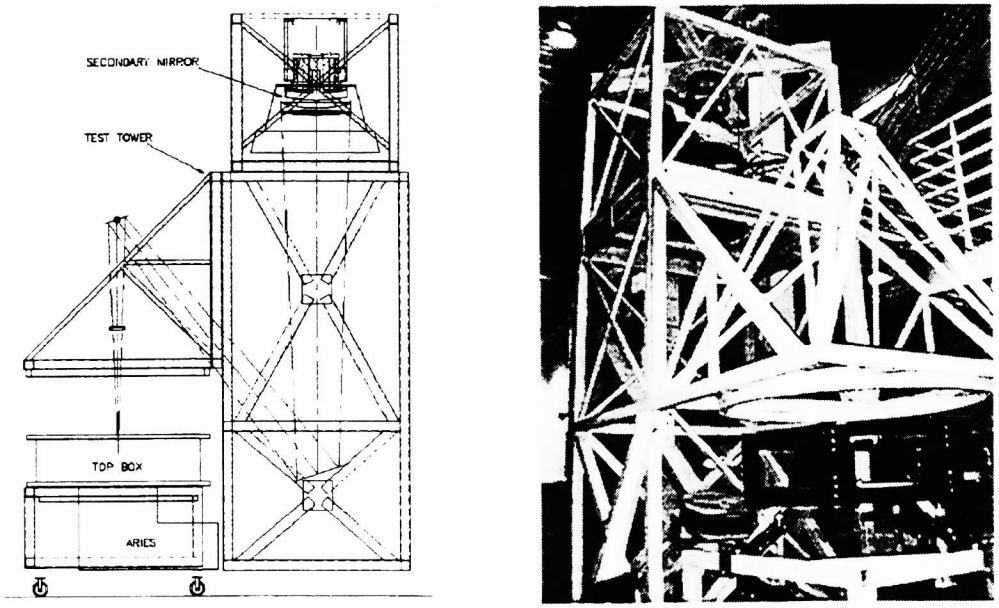

Figure 9. The Shimmulator test tower. The schematic on the left highlights the 9.5m folded optical path and the relationship of the test path within the MMT wavefront sensing Top Box optics, and ARIES, the near infrared science instrument. The photo on the right gives the reader a sense of proportion by comparing the man kneeling at the top near the secondary mirror.

Physically, the Shimmulator optics are divided into three sections; the large two lenses (immediately before the test surface), the doublet and beamsplitter combination and the remaining source and interferometer. All optics are located within the Top Box, except for the two large lenses. These lenses will be installed and removed within the telescope with the aid of a crane when the MMT is in a horizontal position. The doublet and beamsplitter are mounted on a common shaft that rotates in the axis of the telescope for testing and out of the axis of the telescope for observing. The source optics and interferometer are stationary and housed within the Top Box structure. Figure 10 highlights the optical paths within the Top Box optical platform. We expect the process of installing the test optics to take less than 30 minutes if the alignment is repeatable to within the expected tolerances.

An important aspect of the Shimmulator is to correctly map the secondary mirror to the wavefront sensor. Since the wavefront sensor is conjugate to the test surface, the commanded actuator signals must correctly influence the adaptive secondary for proper wavefront reconstruction. The use of fiducials, temporary physical coordinates on the mirror, will be mapped and measured with the interferometer measuring the mapping through the optics. By controlling the spacing of the doublet axially, this mapping can be adjusted to within the defined tolerance.

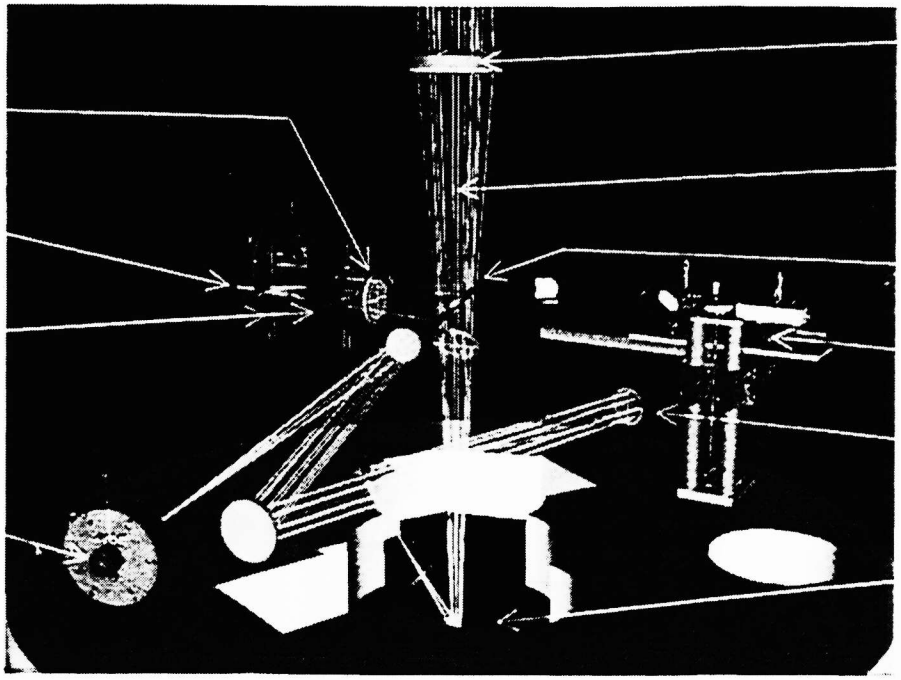

Figure 10. Integration of Shimmulator and interferometer within the Top Box. The wavefront sensing optics parallel with the optics bed is fed visible light reflected off the near infrared dewar window. Under a secondary test situation, the Shimmulator doublet and pair of dichroic beamsplitters are swung into the vertical beam path for calibration and interferometric testing. Removing the doublet and pair of beamsplitters (and the large lenses not pictured) is all that is needed to ready the telescope for observing.

4. IMPLEMENTATION

Although the Shimmulator has relatively few optical elements, the system alignment is quite complex due to the extreme size and tight mechanical tolerances. For example, the spacing between the doublet and the large lenses is over 9m with a tolerance of ±1.5mm. The decentration tolerance of the doublet to the optical axis is less than 50μm. The tip/tilt of the CGH substrate is less than 100μm of total indicator runout and the tilt of the lenses is less than 0.07 degrees with a decentration better than 0.4mm. Although the alignment task has not been trivial, it has been aided greatly with the use of a 10 arcsecond Brunsen focusing alignment telescope and the use of the computer generated hologram alignment patterns. Five CGH were written for the alignment of spacing and tip/tilt of the CGH to the fiber source, the spacing and tip/tilt of the CGH to the small doublet and the decentration of the CGH to the large lens pair. In combination, two concentric alignment rings were etched into the surfaces of both lens pairs so that the projected alignment marks could be matched to the optical centers of the lenses. Initial laboratory tests of computer generated hologram alignment patterns indicated that visual perception can resolve spacing accuracy of around 35 microns due to the interference pattern and intensity pattern.

The use of the CGH alignment spots has been of worthwhile assistance in the alignment of the optical components. However, ironically, the CGH substrate was not written on the substrate provided and was delivered on another substrate less than half the designed thickness. This change in design coupled with an error in the proper surface of alignment scribes etched onto the doublet has actually increased the accuracy of alignment. Although the distance measurement was changed, the CGH four alignment spots are projected diverging and encompass the scribe mark of the doublet. Rather than only one spot that must be centered inside a ring, we now have four spots that are equally centered around the etched scribe mark. Placing a 50x loop on the face of the doublet, we estimate that we can center the doublet to the projected optical axis better than 50μm. The use of alignment spots has allowed us to align the system to within the given tolerances without relying on interferometer feedback.

At the present time, the Shimmulator and interferometer have been aligned to approximately 8 waves peak-to-valley wavefront aberration, better than the expected estimated performance. This is due to the aid of the interferometer in aligning the optics better than the budgeted allowance. The remaining wavefront aberration is the residual from manufacturing errors. Presently we are measurement limited by the vibration in the test tower and attempting to dampen the system. We are looking

at increasing our phase shifting frame rate. This week the optical alignment team will be installing the Top Box optics with the Shack Hartmann wavefront sensor detector and completing the full optical design installation. For initial tests we are placing science cameras at the various focal planes within the Top Box to measure the power spectrum.

5. COMING ATTRACTIONS

The next procedures of the optical system will be to measure the imparted static wavefront turbulence and then the dynamic wavefront turbulence. The interferometer will be able to quantify the atmospheric turbulence plates ability to impart Kolmogorov turbulence. In three months, we will receive the fully adaptive spherical secondary mirror which we will test its ability to compensate for its own shape under the influence of gravity and eventually the atmosphere, both static and dynamic. Once these tests are completed we will install the final adaptive aspheric shell and similarly test the system. The test tower we be shipped to the telescope site where we will again run through the tests off telescope and eventually within the telescope itself. First light for the adaptive secondary is scheduled for early 2000.

ACKNOWLEDGMENTS

A project of this magnitude is not possible without many people's assistance. We would like to thank the numerous Steward Observatory managers, scientists, engineers and support staff for their assistance.

This project has been sponsored by the Air Force Office of Scientific Research under grant #F49620-94-1-0437 and grant #F49620-96-1-0366.

REFERENCES

[1] J.C. Shelton, M. Lloyd-Hart, J.R.P. Angel and D.G. Sandler, "The 6.5m MMT laser-guided adaptive optics system: Overview and progress report II," Proc. SPIE **3126**, p. 2, 1997.

[2] R.J. Sarlot and J.H. Burge, "Optical system for closed-loop testing of the adaptive optic convex mirror," Proc. SPIE **3430**, p. 126, 1998.

[3] T.A. Rhoadarmer, J.R.P. Angel, S.M. Ebstein, M. Lloyd-Harft, M.A. Kenworthy, I. Lanum, M.L. Rademacher, B.C. Fitz-Patrick, and P.C. McGuire, "Design, construction, and testing of a low-cost, broadband static phase plate for generating Kolmogorov turbulence," (to be published), 1999.

[4] B.L. Stamper, "Shimmulator interferometer source for the multiple mirror telescope upgrade," University of Arizona/Steward Observatory internal document, (June 1999).

[5] C. Zhao, "Description of the AO interferometer," ," University of Arizona/Steward Observatory internal document, (May 1999).

[6] R.J. Sarlot, D.W. McCarthy, J.H. Burge, and J. Ge, "Optical design of ARIES: the new near infrared science instrument for the adaptive f/15 Multiple Mirror Telescope", Proc. SPIE **3779**, 1999.

[7] D.W. McCarthy, J.H. Burge, J.R.P. Angel, J. Ge, R.J. Sarlot, B.C. Fitz-Patrick, and J.L. Hinz, "ARIES: Arizona infrared imager and Echelle spectrograph," Proc. SPIE **3354**, p.750, 1998.